Radiative decay of helium doubly excited states

Chien-Nan Liu,[1] Ming-Keh Chen,[2] and C. D. Lin[1]

[1]*Department of Physics, Cardwell Hall, Kansas State University, Manhattan, Kansas 66506*
[2]*Department of Physics, National Chung-Hsin University, Taichung, Taiwan 40227*
(Received 11 January 2001; published 31 May 2001)

A theoretical study of the radiative decay of low-lying doubly excited $^1P^o$ states of Helium in the energy region below the He$^+(N=2)$ threshold is presented. We calculated the oscillator strength from the ground state, the Auger and radiative decay rates, and the natural widths of these states. These rates are used to obtain the photon emission and metastable atom yield spectra to compare with experimental measurements, including those from Odling-Smee *et al.* [Phys. Rev. Lett. **84**, 2598 (2000)] and Rubensson *et al.* [Phys. Rev. Lett. **83**, 947 (1999)]. We showed that the lifetimes of the long-lived doubly excited states are determined by the radiative rates.

PACS number(s): 32.70.Cs, 32.80.Dz

Helium is the prototype system for the study of electron correlation. Manifestations of doubly excited states as resonances in the photoionization spectra have been studied extensively since the pioneering experimental work by Madden and Codling [1] and the corresponding theoretical work by Cooper, Fano, and Prats [2]. Over the last few decades, a detailed understanding of these states has been achieved. Advances in synchrotron light sources and experimental techniques continue to improve the resolution of experimental spectra, thus uncovering weaker features that were not resolved before [3]. On the theoretical front, various approximate quantum numbers have been proposed and adopted to describe these states [4–6], and propensity rules for radiative and nonradiative transitions [7,8] have been discussed.

Most of the previous theoretical and experimental studies of helium doubly excited states assume that the Auger process dominates the decay mechanism, thus considering ion (or photoelectron) yield spectra as a measure of the photoabsorption probability. Note that the natural width of a resonance is proportional to the sum of the Auger decay rate Γ_a and the radiative decay rate Γ_r. Along a given Rydberg series, Γ_a is proportional to $1/(n-\delta)^3$, where δ is the quantum defect [9]. In contrast, radiative decay rate Γ_r stays nearly constant along the series since the radiative decay of a doubly excited state is primarily due to the $2p \rightarrow 1s$ transition of the inner electron. For the He$^+$ ion this lifetime is 0.1 ns.

Continuing progress in synchrotron light sources in the last few years has now offered experimentalists the opportunity to examine the radiative decays of the helium doubly excited states [10–15]. These experiments fall into two groups. One measured the VUV photon yield and the other measured the yields of metastable helium atoms and VUV photon, as a function of the energy of the synchrotron light. Despite the rich literature on doubly excited states of helium, few theoretical calculations on the radiative decay of doubly excited states have been made [16]. In this Rapid Communication we present the radiative rates of the low-lying doubly excited $^1P^o$ states of helium below the He$^+(N=2)$ threshold. From the calculated Auger and radiative decay rates the natural widths of these states are obtained. By following the radiative decay branches of individual doubly excited states, including all the cascade transitions, we derive the expected

VUV photon yields and the metastable atom yields. These data serve to compare with the recent experimental measurements [11,12,14]. In considering the radiative transitions, we treat each doubly excited state as a bound state. A more complete treatment by including the Auger and the radiative transitions coherently is not being done here [17].

In order to obtain the radiative rates of the doubly excited $^1P^o$ states of He below the He$^+(N=2)$ threshold, we calculated the f values for transitions to the singly excited ^1S and ^1D states. The wave functions of the singly excited states have been calculated using the Rayleigh-Ritz variational method with B-spline functions [18]. The wave functions of the doubly excited $^1P^o$ states are obtained by a saddle-point complex rotation method with B-spline functions [19]. In a configuration interaction scheme, we constructed the wave functions in terms of B splines of order k and total number N, defined between two end points, and built vacancies into the wave functions. The B-spline basis functions with an exponential knot sequence [20,21] are employed in the present calculation. We included six lowest partial waves in calculating the saddle-point wave functions of the doubly excited $^1P^o$ states. We ensured that the f values are accurate within the first three digits as the number of partial waves and basis functions increase. Resonance energies and Auger rates have been reported previously [19]. Detailed comparisons of resonance energies and Auger rates with previous work can also be found there.

The doubly excited states are labeled using the $(K,T)_n^A$ classification scheme [4]. Table I documents the main results for each doubly excited state calculated. The second column gives the oscillator strength from the ground state. The third column gives the total Auger rate, and the fourth and fifth columns give the total radiative rates to the ^1S singly excited states and to the ^1D singly excited states, respectively. For each higher doubly excited state with principal quantum number n, the transitions tend to decay to $1sns$ and $1snd$ states. The sixth column gives the total radiative rate. The total decay rate for each doubly excited state is given in the last column. Only doubly excited states below the He$^+(N=2)$ threshold for $n \leq 7$ are considered.

From this table, we notice the well-known fact that the Auger rates for the $(0,1)_n^+$ series are about two orders of

TABLE I. Oscillator strength from the ground state f, Auger decay rate Γ_a, and radiative decay rates $\Gamma_{r,s}$ and $\Gamma_{r,d}$ corresponding, respectively, to transitions into ^1S and ^1D singly excited states for doubly excited states $(K,T)_n^a$. $\Gamma_r = \Gamma_{r,s} + \Gamma_{r,d}$ is the total radiative decay rate. $\Gamma = \Gamma_r + \Gamma_a$ is the total decay rate. All decay rates are shown in units of s^{-1}. Numbers in square brackets indicate powers of 10.

State	f	Γ_a	$\Gamma_{r,s}$	$\Gamma_{r,d}$	Γ_r	Γ
$(0,1)_2^+$	6.98[−3]	5.70[13]	6.66[9]	0.28[9]	6.94[9]	5.71[13]
$(0,1)_3^+$	1.14[−3]	1.24[13]	5.65[9]	1.57[9]	7.22[9]	1.24[13]
$(0,1)_4^+$	4.60[−4]	0.53[13]	5.60[9]	1.92[9]	7.52[9]	5.31[12]
$(0,1)_5^+$	2.30[−4]	0.26[13]	5.60[9]	2.07[9]	7.67[9]	2.61[12]
$(0,1)_6^+$	1.32[−5]	0.15[13]	5.69[9]	2.07[9]	7.76[9]	1.55[12]
$(0,1)_7^+$	8.25[−5]	0.92[12]	5.70[9]	2.10[9]	7.80[9]	9.28[11]
$(1,0)_3^-$	2.87[−5]	1.60[11]	4.70[9]	0.63[9]	5.33[9]	1.65[11]
$(1,0)_4^-$	2.18[−5]	0.84[11]	3.20[9]	4.17[9]	7.37[9]	9.14[10]
$(1,0)_5^-$	1.11[−5]	0.41[11]	3.40[9]	4.48[9]	7.88[9]	4.89[10]
$(1,0)_6^-$	6.15[−6]	2.24[10]	3.60[9]	4.69[9]	8.29[9]	3.07[10]
$(1,0)_7^-$	3.73[−6]	1.33[10]	3.67[9]	4.87[9]	8.54[9]	2.18[10]
$(-1,0)_3^0$	2.49[−6]	0.62[9]	8.76[8]	3.34[9]	4.22[9]	4.84[9]
$(-1,0)_4^0$	2.22[−6]	1.24[8]	6.29[8]	3.14[9]	3.77[9]	3.89[9]
$(-1,0)_5^0$	1.46[−6]	0.63[8] [a]	5.39[8]	3.00[9]	3.54[9]	3.60[9]
$(-1,0)_6^0$	9.67[−7]	0.37[7] [a]	0.89[8]	2.89[9]	2.98[9]	3.02[9]

[a]Estimated

magnitude larger than the corresponding states of the $(1,0)_n^-$ series, and the Auger rates for the latter are two orders higher than the corresponding states of the $(-1,0)_n^0$ series. The Auger rates for the higher members of the $(-1,0)_n^0$ series are so small, in fact, that we obtained the Auger rates for $n=5$ and 6 by estimate following the $1/n^{*3}$ rule, where n^* is the effective principal quantum number. Since the Auger rates for these states in the $(-1,0)_n^0$ series are much smaller than the radiative rates, error in the estimate is not important.

From Table I we also note that the radiative rates for all the doubly excited states are of the same order. They are to be compared with the radiative decay rate of $1.0 \times 10^{10}\,s^{-1}$ for the $2p \to 1s$ transition of He^+. By comparing the Auger and radiative rates, the lifetimes of the lower states of the $(0,1)_n^+$ series are clearly determined by the Auger rates. Again using the $1/n^{*3}$ rule, we expect the Auger and the radiative rates to become comparable for the $(0,1)_n^+$ series at $n \approx 30$. For the $(1,0)_n^-$ series, the radiative rates for small n are not as large as the Auger rates, but they are not negligible. The simple $1/n^{*3}$ rule would give the two equal rates at $n \approx 8$. The most interesting result of Table I is the radiative rates of the $(-1,0)_n^0$ series. This series is not easily excited by single-photon absorption and decays predominantly by photon emission. This is already true for the lowest $n=3$ member of this series. From the calculated rates we note that the $(-1,0)_3^0$ state (called $2p3d$ by some authors) has a lifetime of 207 ps. The higher members have lifetimes of 257 ps, 278 ps, and 331 ps, according to our calculation. Such long lifetimes probably can be determined directly from time
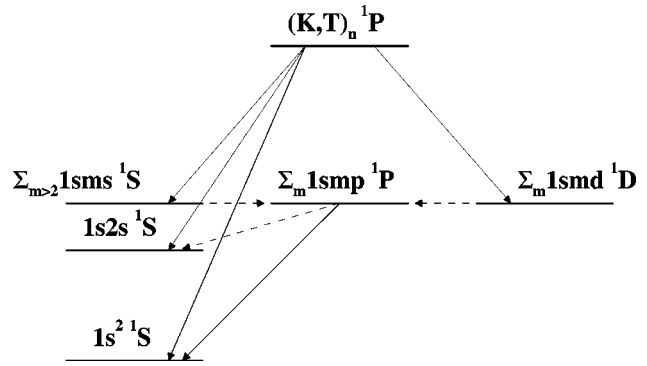

FIG. 1. Schematic diagram of the radiative decay scheme. Transitions that produce VUV photons are shown in solid lines. Other possible transitions are shown in dashed lines.

measurements. We comment that our predicted width of 3.17 μeV for the lowest $(-1,0)_3^0$ state is in good agreement with a recent experimental study, which measured the time delay of the fluorescent decay and determined a lower limit for the width of 3.30 μeV [15].

Closer examination of the results presented in Table I reveals information regarding configuration interaction. The three $^1P^o$ series converging to $He^+(N=2)$, $(0,1)^+$, $(1,0)^-$, and $(-1,0)^0$, are also alternatively described approximately by configuration classifications, $2snp \pm 2pns$ and $2pnd$, which characterize the leading configuration components. As the configurations might suggest, it is commonly assumed that radiative decay rates for these states can be described by the dominant $2p \to 1s$ transition, which has a rate of $1.0 \times 10^{10}\,s^{-1}$. However, all the radiative decay rates, Γ_r, presented in Table I, are smaller, reflecting the importance of configuration interaction and the failure of single configuration representation for these states. Note that the total rates for the $(-1,0)_n^0$ states are less than half the rate of the $He^+(2p)$ state. Nevertheless, $(-1,0)_n^0$ states preferentially decay into $1smd$ states with a branching ratio of about 80%, showing their dominant $2pnd$ configurations. Although $(0,1)_n^+$ and $(1,0)_n^-$ states are both described by linear combinations of $2snp$ and $2pns$, their radiative decay rates reveal more complex configuration interactions. While the $(0,1)_n^+$ states preferentially decay into $1sms$ states, the $(1,0)_n^-$ states have comparable branching ratios into $1sms$ and $1smd$ states. Therefore, $(1,0)_n^-$ states have relatively larger $2pnd$ configurations. It is interesting to point out that the sum of the radiative rates of the three $(K,T)_n$ states with the same n is roughly twice the radiative rate for the He^+ $2p \to 1s$ transition. While only the $2pns$ and $2pnd$ have significant radiative decay rates to $1sns$ and $1snd$, respectively, the radiative decay rate of $2snp$ to $1snl$ would be much weaker.

Radiative decay of a doubly excited state can proceed through several different paths as shown by a schematic diagram in Fig. 1. A direct radiative decay into the ground state results in emission of a single VUV photon. The other one-step process is a radiative decay into the $1s2s\,^1S$ state, producing a VUV photon and a metastable atom. Radiative decays into other $1sns\,^1S$ and $1snd\,^1D$ states will be followed

TABLE II. Metastable atom and VUV photon yields from fluorescence decay of the doubly excited states $(K,T)_n^A$ ordered according to increasing excitation energies.

State	Metastable atom yield	Photon yield
$(0,1)_2^+$	7.92×10^3	9.89×10^3
$(1,0)_3^-$	5.18×10^3	1.47×10^4
$(0,1)_3^+$	4.72×10^1	1.42×10^4
$(-1,0)_3^0$	1.15×10^3	4.57×10^4
$(1,0)_4^-$	5.30×10^2	3.74×10^4
$(0,1)_4^+$	6.39×10^1	1.40×10^4
$(-1,0)_4^0$	5.58×10^2	4.62×10^4
$(1,0)_5^-$	3.60×10^2	3.83×10^4
$(0,1)_5^+$	9.16×10^1	1.43×10^4
$(-1,0)_5^0$	2.79×10^2	3.09×10^4
$(1,0)_6^-$	2.90×10^2	3.56×10^4
$(0,1)_6^+$	1.01×10^2	1.42×10^4
$(-1,0)_6^0$	1.15×10^2	2.08×10^4
$(1,0)_7^-$	2.40×10^2	2.13×10^4
$(0,1)_7^+$	1.12×10^2	1.48×10^4

by cascade fluorescence decay through $1smp\ {}^1P^o$ $(m<n)$ states into either the $1s^2$ or $1s2s\ {}^1S$ state, since these $1snl$ singly excited states are generally short-lived. Therefore, summing over one-step and cascade processes and neglecting those of higher order, the VUV photon yield intensity F_n and the metastable atom yield M_n from a given doubly excited state n can be described by the following formulas.

$$F_n = f_n \left[\sum_i \frac{c_i + d_i}{\Gamma} + \sum_{i>2,j} \frac{c_i}{\Gamma} P_{ij} Q_{j1} + \sum_{i,j} \frac{d_i}{\Gamma} R_{ij} Q_{j1} \right], \quad (1)$$

$$M_n = f_n \left[\frac{c_2}{\Gamma} + \sum_{i>2,j} \frac{c_i}{\Gamma} P_{ij} Q_{j2} + \sum_{i,j} \frac{d_i}{\Gamma} R_{ij} Q_{j2} \right], \quad (2)$$

where f_n is the oscillator strength from the ground state to the state n, $\Gamma = \Gamma_a + \Gamma_r$ is the total decay rate, c_i and d_i are the radiative decay rates to the $1sis\ {}^1S$ and $1sid\ {}^1D$ states, respectively, obtained from the present calculations, P_{ij} and R_{ij} are the fluorescence branching ratios corresponding to $1sis \rightarrow 1sjp$ and $1sid \rightarrow 1sjp$ transitions, respectively, and Q_{ij} is the fluorescence branching ratio from $1sip$ to $1sjs$. These branching ratios for singly excited states are known in the literature [22]. For example, Q_{i1} is approximately 97% and Q_{i2} is about 3%. Note that $\Sigma_i c_i = \Gamma_{r,s}$ and $\Sigma_i d_i = \Gamma_{r,d}$ (cf. Table I). Single excited states $1snl$ with high n are also metastable, but they are not included in Eq. (2) due to their negligible contributions. Radiative decays through lower doubly excited states are not included because they involve much smaller transition energies. Our calculations show that only three of the states reported here have radiative decay rates to lower doubly excited states that exceed 1% of their total radiative decay rates to singly excited states.

Results for metastable atom and VUV photon yields are presented in Table II. Since both $\Sigma_j P_{ij} Q_{j1}$ and $\Sigma_j R_{ij} Q_{j1}$ are close to unity,

TABLE III. Relative peak intensities of metastable atom yields (MY) and VUV photon yields (FY). The present results correspond to the peak values of the convoluted resonance profiles in the fluorescence spectra. The results are normalized with respect to the sum for the two states, $(-1,0)_3^0$ and $(1,0)_1^4$.

	MY		FY	
State	Expt. [a]	This work	Expt. [a]	This work
$(0,1)_2^+$	147(24)	344.3	. . .	8.7
$(0,1)_3^+$	15(4)	2.6	17(14)	16.0
$(0,1)_4^+$	17(3)	3.7	24(4)	16.4
$(0,1)_5^+$	15(3)	5.4	26(6)	17.0
$(1,0)_3^-$	208(8)	309.5	45(6)	17.8
$(-1,0)_3^0$ and $(1,0)_4^-$	100	100	100	100
$(-1,0)_4^0$ and $(1,0)_5^-$	49(3)	54.7	73(6)	101.9
$(-1,0)_5^0$ and $(1,0)_6^-$	37(3)	33.9	58(7)	80.3

[a]Reference [11].

$$F_n \approx 2 f_n \frac{\Gamma_r}{\Gamma} - f_n \frac{c_1 + c_2}{\Gamma}. \quad (3)$$

Since the fluorescence branching ratio is quite small for the $(0,1)_n^+$ series, this equation explains the weak VUV photon yields for the $+$ series. However, it is not easy to identify a particular tendency in metastable atom yields. For example, the $(0,1)_2^+$ state produces the largest metastable atom yield, resulting from the combination of a large oscillator strength from the ground state and the dominance of the transition to $1s2s$ state among all radiative channels, although the branching ratio for radiative decay is only 0.12%. Generally, radiative decay proceeds preferentially via $(K,T)_n^A \rightarrow 1sms$ (or $1smd$) for $m=n$. Therefore, except for $(0,1)_2^+$ and $(1,0)_3^-$, the metastable atom yields are dominated by cascade processes. Since Q_{j2} is almost two orders of magnitude smaller than Q_{j1} for these cases, the photon yields are also two orders of magnitude larger than the corresponding metastable atom yields.

Our results are compared to two recent measurements in Tables III and IV. To compare with the measurements of Odling-Smee et al. [11], the Lorentzian resonance profiles in the metastable atom yield (MY) and VUV photon yield (FY) spectra have to be convoluted with a Gaussian envelope with

TABLE IV. Relative peak intensities of VUV photon yields. The present results correspond to the peak values of the convoluted resonance profiles in the fluorescence spectra. The results are normalized with respect to the $(-1,0)_3^0$ state.

State	Experiment [a]	Present results
$(-1,0)_3^0$	1.0	1.0
$(1,0)_4^-$	0.54	0.81
$(-1,0)_4^0$	0.44	1.01
$(1,0)_5^-$	0.21	0.84
$(-1,0)_5^0$	0.12	0.68
$(1,0)_6^-$	0.09	0.78

[a]Reference [12].

a width corresponding to the energy resolution of 60 meV for the incoming photon, which is larger than the spacing between $(-1,0)_n^0$ and $(1,0)_{n+1}^-$, and several orders of magnitude larger than the natural widths of the states. As a result, the peak intensities of the measured Lorentzian profiles are proportional to the combined yield from the two states. Table III shows good qualitative agreement on *metastable atom* yields between experiment and present results. On the other hand, the comparison of VUV *photon* yields shows less agreement.

For the discrepancies in VUV photon yields, we have to point out that the photon yields from the two measurements [11,12] are not consistent with each other. As seen from Table IV, the relative peak intensities from the data of Rubensson *et al.* [12], which were taken at a resolution of 3–7 meV, do not agree with the relative peak intensities of the convoluted theoretical results presented in this table. We point out that our calculated results appear to be in good agreement with a recent measurement [14], which has a better energy resolution to resolve fluorescence profiles corresponding to $(-1,0)_n^0$ and $(1,0)_{n+1}^-$ $^1P^o$ states up to $n=6$.

In conclusion, we have presented a theoretical study for the radiative decay of low-lying doubly excited $^1P^o$ states of helium below the $He^+(N=2)$ threshold, including calculations for Auger and radiative decay rates, predictions for metastable atom and VUV photon yields in the fluorescence spectra, and comparisons between our results with experimental measurements. The radiative decay rate of individual doubly excited states reflects the importance of configuration mixing. Neglected by most prior studies, radiative decay is shown to be more important than autoionization in the decay mechanism of some doubly excited states. Among the low-lying states, the $(-1,0)_n^0$ series decays predominantly via radiative channels, while the Auger process dominates the decay of $(0,1)_n^+$ and $(1,0)_n^-$ series. With increasing brightness available from synchrotron radiation sources, it is becoming possible to examine the radiative branch of the decay of doubly excited states of helium. These data would provide critical information on those doubly excited states that have so far been neglected both theoretically and experimentally.

[1] R. P. Madden and K. Codling, Phys. Rev. Lett. **10**, 516 (1963).

[2] J. W. Cooper, U. Fano, and F. Prats, Phys. Rev. Lett. **10**, 518 (1963).

[3] See, for example, M. Domke, K. Schulz, G. Remmers, G. Kaindl, and D. Wintgen, Phys. Rev. A **53**, 1424 (1996), and references therein.

[4] C. D. Lin, Phys. Rev. A **29**, 1019 (1984); Adv. At. Mol. Phys. **22**, 77 (1986).

[5] D. R. Herrick, Phys. Rev. A **12**, 413 (1975); Adv. Chem. Phys. **52**, 1 (1983).

[6] J. M. Feagin and J. S. Briggs, Phys. Rev. Lett. **57**, 984 (1986); Phys. Rev. A **37**, 4599 (1988).

[7] J. M. Rost and J. S. Briggs, J. Phys. B **23**, L339 (1990); A. Vollweiter, J. M. Rost, and J. S. Briggs, *ibid.* **24**, L115 (1991).

[8] H. R. Sadeghpour and C. H. Greene, Phys. Rev. Lett. **65**, 313 (1990).

[9] U. Fano and J. W. Cooper, Phys. Rev. **137**, A1364 (1965).

[10] E. Sokell, A. A. Wills, P. Hammond, M. A. MacDonald, and M. K. Odling-Smee, J. Phys. B **29**, L863 (1996).

[11] M. K. Odling-Smee, E. Skoell, P. Hammond, and M. A. MacDonald, Phys. Rev. Lett. **84**, 2598 (2000).

[12] J.-E. Rubensson, C. Såthe, S. Cramm, B. Kessler, S. Stranges, R. Richter, M. Alagia, and M. Coreno, Phys. Rev. Lett. **83**, 947 (1999).

[13] T. W. Gorczyca, J.-E. Rubensson, C. Såthe, M. Ström, M. Agaker, D. Ding, S. Stranges, R. Richter, and M. Alagia, Phys. Rev. Lett. **85**, 1202 (2000).

[14] F. Penent, P. Lablanquie, R. I. Hall, M. Zitnik, K. Bucar, S. Stranges, R. Richter, M. Alagia, P. Hammond, and J. Lambourne (unpublished).

[15] J. G. Lambourne, M. K. Odling-Smee, J. R. Harries, P. Hammond, S. Stranges, M. Ferianis, R. Richter, and M. Coreno (unpublished).

[16] H. O. Dickinson and M. R. H. Rudge, J. Phys. B **3**, 1284 (1970).

[17] F. Robicheaux, T. W. Gorczyca, M. S. Pindzola, and N. R. Badnell, Phys. Rev. A **52**, 1319 (1995).

[18] M.-K. Chen, J. Phys. B **26**, 3025 (1993); **27**, 865 (1994); **26**, 4847 (1994).

[19] M.-K. Chen, Phys. Rev. A **56**, 4537 (1997).

[20] M.-K. Chen and C.-S. Hsue, J. Phys. B **25**, 4059 (1992).

[21] W. R. Johnson, S. A. Blundel, and J. Sapirstein, Phys. Rev. A **37**, 307 (1988).

[22] C. E. Theodosiou, At. Data Nucl. Data Tables **36**, 97 (1987).